

# Direct Detection and Reactivity of the Short-Lived Phenyloxenium Ion

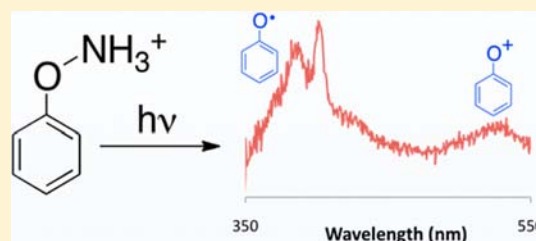
Patrick J. Hanway,<sup>†</sup> Jiadan Xue,<sup>‡</sup> Ujjal Bhattacharjee,<sup>†</sup> Maecia J. Milot,<sup>†</sup> Zhu Ruixue,<sup>‡</sup> David Lee Phillips,<sup>‡</sup> and Arthur H. Winter\*<sup>†</sup>

<sup>†</sup>Department of Chemistry, Iowa State University, 2101d Hach Hall, Ames, Iowa 50011, United States

<sup>‡</sup>Department of Chemistry, The University of Hong Kong, Pokfulam Road, Hong Kong, People's Republic of China

## Supporting Information

**ABSTRACT:** Photolysis of protonated phenylhydroxylamine was studied using product analysis, trapping experiments, and laser flash photolysis experiments (UV–vis and TR<sup>3</sup> detection) ranging from the femtosecond to the microsecond time scale. We find that the excited state of the photoprecursor is followed by two species: a longer-lived transient (150 ns) that we assign to the phenoxy radical and a shorter-lived (3–20 ns) transient that we assign to the singlet phenyloxenium ion. Product studies from photolysis of this precursor show rearranged protonated *o*-/*p*-aminophenols and solvent water adducts (catechol, hydroquinone) and ammonium ion. The former products can be largely ascribed to radical recombination or ion recombination, while the latter are ascribed to solvent water addition to the phenyloxenium ion. The phenyloxenium ion is apparently too short-lived under these conditions to be trapped by external nucleophiles other than solvent, giving only trace amounts of *o*-/*p*-chloro adducts upon addition of chloride trap. Product studies upon thermolysis of this precursor give the same products as those generated from photolysis, with the difference being that the *ortho* adducts (*o*-aminophenol, hydroquinone) are formed in a higher ratio in comparison to the photolysis products.



## INTRODUCTION

Oxenium ions are reactive species with the formula R–O<sup>+</sup>. As isoelectronic analogues of nitrenes, oxenium ions are strong hypovalent electrophiles with a formally positive charge on an electronegative oxygen. As we have detailed elsewhere,<sup>1,2</sup> these species have been proposed in a number of useful *unpolung* synthetic transformations, such as electrochemical oxidations of phenols and phenolates,<sup>3,4</sup> alkane oxidations,<sup>5</sup> and a wide variety of other phenolic oxidations and tautomerization reactions.<sup>6–10</sup> Many of these reactions convert feedstock phenols and alkanes into value-added products such as substituted phenols, oxidized alkanes, and cyclohexadienones as well as petrochemicals such as poly(1,4-phenylene ether), a high-value industrial thermoplastic.<sup>11–13</sup> Like nitrenes and carbenes, oxenium ions are short-lived in solution but can form stable complexes with transition metals, acting as interesting ligands.<sup>14</sup> These species also have relevance to astrochemistry, as aryloxenium ions are formed from exposing phenols, anisoles, and nitrobenzenes to ionizing radiation,<sup>15–17</sup> and oxenium ions can persist in interstellar clouds and planet atmospheres.<sup>18–20</sup> Of biological relevance, some aryloxenium ions are proposed to be reactive intermediates in iron-mediated enzymatic oxidations of phenols into quinone compounds.<sup>21</sup> Given the diverse applicability of these species, it is surprising how very little is known about this class of reactive intermediates.

A major roadblock that has stymied the detailed study of oxenium ions is the lack of suitable photoprecursors to these

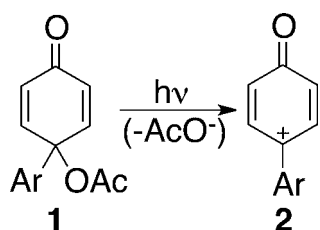
ions. Studies of related intermediates such as carbenes,<sup>22,23</sup> nitrenes,<sup>24–26</sup> and nitrenium ions<sup>27–29</sup> have benefited tremendously from the ability to generate these species photochemically from established precursors (e.g., aryl azides, diazo compounds, etc.), permitting detailed spectroscopic studies of their reactivity and properties. In contrast, there are few photoprecursors to oxenium ions. Some reports suggest oxenium ions can be formed as part of intermediate mixtures from multiphoton ionization studies or from mass spectral ion fragmentations,<sup>17,30–32</sup> but recent attempts at developing robust single-photon precursors to these species suitable for mechanistic studies, by either photolysis or thermolysis, have proven to be challenging.<sup>33–36</sup>

However, in exciting recent studies reported by Novak and Platz, a 4'-methyl-4-biphenyloxenium ion was generated by photolysis of the 4-(4-methylphenyl)-4-acetoxy cyclohexadienonyl derivative (shown in Scheme 1).<sup>34,37</sup> These studies were significant because they demonstrated the direct observation of a discrete oxenium ion using laser photolysis. This photoprecursor has the limitation that it requires a *para* substituent to prevent tautomerization, making it unsuitable for the photo-generation of the parent phenyloxenium ion.

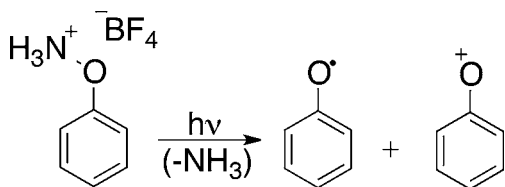
However, it is of considerable interest to understand the reactivity of the phenyloxenium ion, since this species is the parent aryloxenium ion and may allow benchmarking the

Received: April 4, 2013

Published: May 28, 2013

Scheme 1. Previous Example of LFP of the 4'-Methyl-4-biphenyloxenium Ion<sup>38</sup>

reactivity of this class of reactive intermediate in comparison to the related phenylnitrene, phenylnitrenium ion, and phenylcarbene. Thus, to generate the phenyloxenium ion, we required a new photoprecursor. On the basis of a report of *N*-arylhiazirinium ions generating arylnitrenium ions upon photolysis,<sup>39</sup> we considered that **3** might similarly generate the phenyloxenium ion by photolysis, leading to O–N heterolytic scission with ejection of neutral ammonia. A potential advantage of this precursor (Scheme 2) is that it is

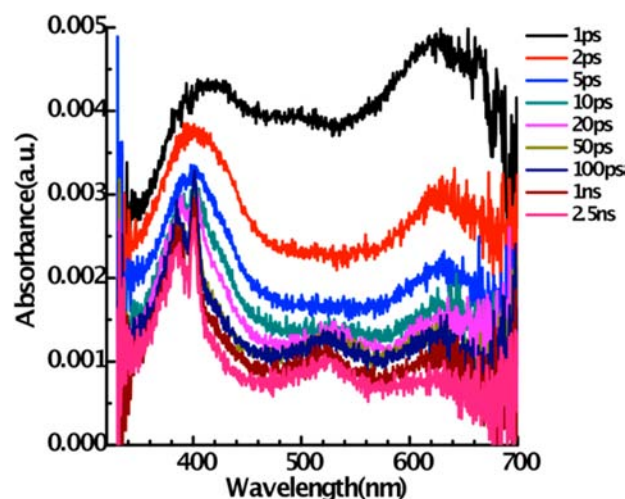
Scheme 2. Proposed Precursor for the Observation of the Phenyloxenium Ion **4**

positively charged rather than neutral, so that in principle the oxenium ion could be generated in any solvent system and would not be restricted to the ionizing solvents necessary for efficient generation of ion pairs from neutral precursors.

On the basis of laser flash photolysis studies ranging from the femtosecond to the microsecond time scale, product analysis, trapping experiments, and computed spectroscopic signatures, we find that photolysis of the protonated phenyl hydroxylamine **3** generates a short-lived intermediate consistent with the phenyloxenium ion as well as a longer-lived phenoxy radical. The putative phenyloxenium ion is too short-lived to be significantly trapped by external nucleophiles other than solvent. The major products from photolysis and thermolysis of this precursor are phenol as well as the rearranged protonated *o*-/*p*-aminophenol and water adducts (hydroquinone, catechol), with photolysis leading to *para* adducts as the major products and thermolysis leading to an increased preference for *ortho* adducts.

## RESULTS AND DISCUSSION

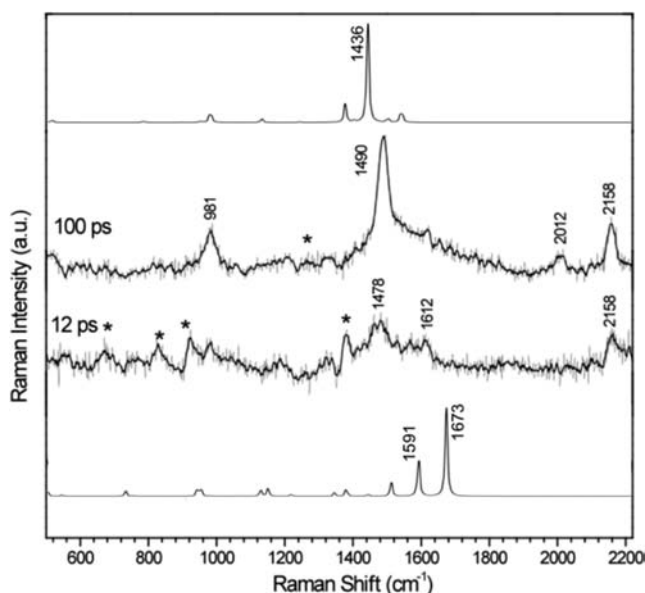
**Laser Flash Photolysis (LFP) of 3.** Photolysis of **3** by LFP was performed in acetonitrile and a mixture of acetonitrile and water (9/1 and 1/1), using 266 nm excitation. The LFP spectra can be seen in Figure 1. A very broad, short-lived transient is observed immediately after the pulse ( $\tau \approx 5$  ps), which we attribute to the excited state of **3**. Two longer-lived transients are also observed at later times after the excitation pulse. The first, having a set of absorptions at  $\sim 400$  nm and a weaker band at 620 nm, can be assigned to the known spectrum of the phenoxy radical ( $\tau = 150$  ns).<sup>40–42</sup> The slight blue shift and sharpening of the bands over  $\sim 30$  ps is characteristic of

Figure 1. LFP spectra of the precursor **3** in acetonitrile.

vibrational cooling, wherein the vibrationally hot radical sheds heat to solvent. The lifetime of this 400 nm transient is not measurably reduced by an added azide trap, as would be expected of a radical and not a cationic species. The other transient is a broad absorption centered around 525 nm (after vibrational cooling) that is short-lived ( $\tau = 3$ –20 ns). We must provide a range for the lifetime of this transient, since the decay falls within the temporal “blind spot” between our femtosecond and nanosecond LFP setups—the decay is too slow to get a proper fit employing our femtosecond system, but the transient is gone within the detection limit ( $\sim 20$  ns) of our nanosecond setup. Unfortunately, having this transient decay within our temporal blind spot makes kinetic studies of this band difficult. However, on the basis of evidence described below, we assign this band to the phenyloxenium ion. Thus, the likely lifetime of this species is  $\sim 5$  ns, with an upper limit on the lifetime of 20 ns, which is the shortest time we can observe with our nanosecond LFP setup.

As further confirmation that the 400 nm transient is the phenoxy radical, we performed LFP experiments with time-resolved resonance Raman (TR<sup>3</sup>) detection. The TR<sup>3</sup> experiments using an incident beam at 400 nm (Figure 2) show a strong peak at 1490 cm<sup>-1</sup>, which correlates to reported values for the phenoxy radical.<sup>41,43</sup> Unfortunately, TR<sup>3</sup> experiments with an incident beam at 532 nm to observe the resonance Raman spectrum of the putative oxenium ion gave no measurable spectrum. Possibly, the extinction coefficients and amounts of the presumed oxenium ion are too low to obtain a measurable spectrum using our experimental setup.

**Assignment of the 525 nm Transient to the Phenyloxenium Ion.** While we were unable to obtain a TR<sup>3</sup> spectrum of the 525 nm transient, a number of pieces of evidence suggest that it is the phenyloxenium ion. First, the laser flash photolysis spectra that we obtain are very similar to those seen for the previously reported 4'-methyl-4-biphenyloxenium ion.<sup>38</sup> Photolysis of the acetyl precursor **1** led to two transients: a long-lived transient at lower wavelength (360 nm) corresponding to a biphenyloxy radical and a shorter-lived transient (170 ns, 460 nm) at higher wavelength corresponding to the 4'-methyl-4-biphenyloxenium ion.<sup>37,38</sup> Our LFP studies give very similar results, with a long-lived band at  $\sim 400$  nm ( $\tau = 150$  ns) that we can definitively assign to the phenoxy radical and a short-lived weakly absorbing band at 525 nm ( $\tau = 3$ –20 ns).



**Figure 2.** ps-KTR<sup>3</sup> spectra at 12 and 100 ps of the precursor **3** along with computed spectra of the phenyloxonium ion (bottom) and the phenoxy radical (top). Asterisks represent solvent subtraction artifacts.

Thus, the 525 nm transient absorption is in a location similar to that for the 4'-methyl-4-biphenyloxonium ion, but with a shorter lifetime ( $\tau = 120$  ns for the 4'-methyl-4-biphenyloxonium ion in water), which would be expected of a less stabilized species.

Second, previous studies have shown that TD-DFT can sometimes provide reasonable estimates of UV-vis spectra for related reactive intermediates.<sup>44–46</sup> Thus, we computed the absorption spectrum of the singlet phenyloxonium ion using TD-B3LYP/6-311+G(2d,p), shown in Figure 3. The computed

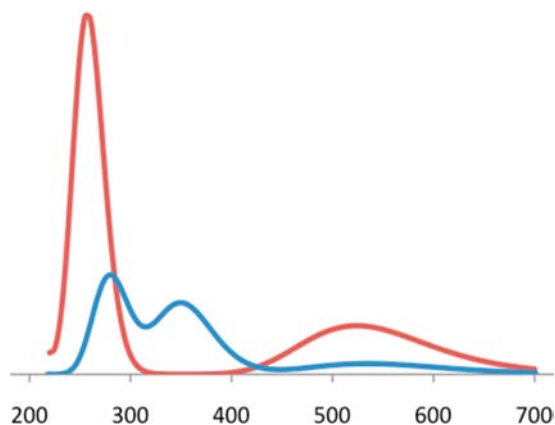


**Figure 3.** Computed UV spectra (TD-B3LYP/6-311+G(2d,p)) of the phenyloxonium ion (red) and the phenoxy radical (blue).

absorption band for **4** gives a single band in the visible region of the UV-vis spectrum centered at 524 nm, in good agreement with the experimental band (see Figure 1).

Third, this 525 nm absorption is quenched as the solvent is changed to mixtures with increasing amounts of water (Figure 4). The band is largest in neat acetonitrile, smaller in 1/1 CH<sub>3</sub>CN/H<sub>2</sub>O, and negligible in 1/9 CH<sub>3</sub>CN/H<sub>2</sub>O. This quenching behavior by nucleophilic water would be expected of a highly electrophilic intermediate. Fourth, product studies

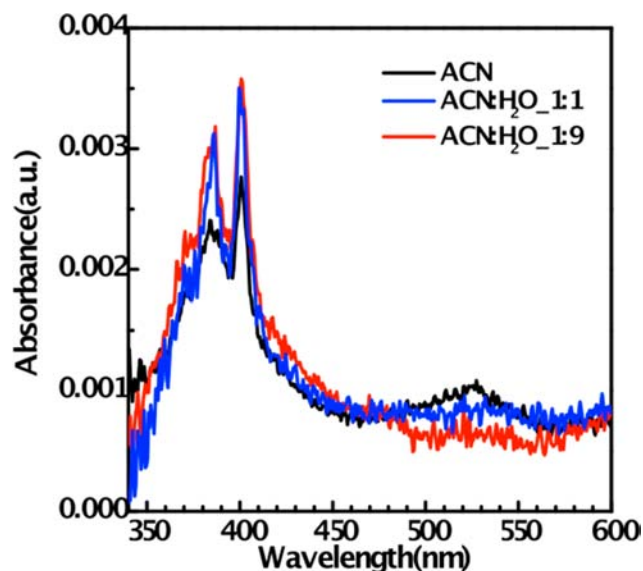


**Figure 4.** LFP spectra of precursor **3** in different solvents obtained at  $\sim 500$  ps.

from photolysis (and thermolysis) of **3** (described below) show small amounts of water adducts that would be expected of a cationic but not a radical intermediate.

Finally, alternative assignments including a triplet excited state of **3** or the triplet oxonium ion **3**<sup>4</sup> seem less likely. Our DFT computations of the triplet excited state of **3** indicates that it is a dissociative state, optimizing to ammonia and the triplet phenyl oxonium ion **3**<sup>4</sup>. Further, our previous computational study indicates that **4** has a closed-shell singlet ground state, which is ca. 20 kcal/mol lower in energy than the lowest energy triplet state, making it less likely to be the triplet phenyloxonium ion.<sup>1</sup> Finally, The triplet oxonium ion **3**<sup>4</sup> is computed by TD-DFT to have major absorptions at 346 and 789 nm, in poor agreement with what we observe. Although in the absence of a TR<sup>3</sup> spectrum it is hard to be definitive, the sum of this evidence leads us to assign this 525 nm band to the singlet phenyloxonium ion.

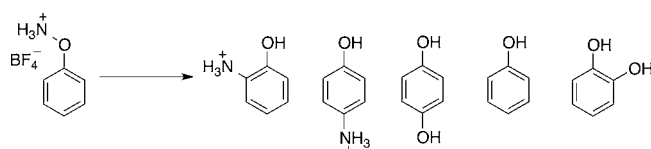
#### Photochemical and Thermal Product Studies of **3**.

Products of the singlet oxonium ion are anticipated to derive from standard two-electron nucleophilic addition chemistry rather than diradical-type chemistry that is often associated with atom-centered triplets, such as the isoelectronic ground-state triplet phenylnitrene. Product studies were performed in different solvent systems, shown in Scheme 3. When the precursor is photolyzed in solvents containing water, the products are a mixture of protonated *o*- and *p*-aminophenol as well as the water adduct hydroquinone. We also see the 1/1/1 triplet at 6 ppm characteristic of the <sup>1</sup>H NMR of the ammonium cation. *ortho* and *para* ring adducts are characteristic of oxonium ions.<sup>33,35,47–51</sup>

The rearranged products could derive either from recombination of the phenoxy radical and ammonia radical cation or from recombination of ammonia with the phenyloxonium ion. The water adduct, hydroquinone, likely derives from water addition to the phenyloxonium ion. Phenol is also obtained in solvents other than water (e.g., neat MeOH, CH<sub>3</sub>CN). Phenol may derive from either the phenoxy radical via a hydrogen atom abstraction process or from the phenyloxonium ion from a hydride transfer process. Addition of chloride as a trap, either in the form of added NaCl to solutions of **3** or from photolysis of



**Scheme 3. Product Studies on the Phenylhydroxylamine Tetrafluoroborate Salt 3<sup>a</sup>**



$h\nu$ $H_2O$	52%	44%	4%	--	--
$h\nu$ $CH_3CN$	38%	29%	--	33%	--
$h\nu$ $MeOH$	40%	20%	--	40%	--
$h\nu$ $CH_3CN/H_2O$ 1:1	53%	42%	5%	--	--
$h\nu$ $MeOH/H_2O$ 1:1	53%	45%	2%	--	--
$\Delta$ , $H_2O$	50%	18%	18%	--	14%

<sup>a</sup>Yields were determined by <sup>1</sup>H NMR integration.

the chloride salt of **3** rather than the  $BF_4^-$  salt, leads to only trace amounts of the *o*-/*p*-chlorophenol as detected by GC-MS. It is possible that ejected ammonia may not undergo cage escape prior to recombination. This result suggests that the phenyloxonium ion is too short-lived to be trapped to a significant extent by externally added nucleophiles other than solvent under these conditions.

The thermolysis of **3** in water gives products similar to those seen from photolysis. The major difference is that the thermolysis products show an increasing preference for forming the *ortho* adducts in comparison to what is found under the photolysis conditions. Thus, larger amounts of *ortho* ammonium phenol are formed as well as catechol along with hydroquinone. One possibility for this increasing preference for formation of the *ortho* adducts could be that the thermolysis conditions are under thermodynamic control. We performed DFT computations of the Wheland  $\sigma$  complex for addition of water and ammonia to the *ortho* and *para* positions. For both the protonated aminophenol and the dihydroxybenzene cases, the *ortho*  $\sigma$  complex was found to be lower in energy than the *para*  $\sigma$  complex. These lower energies could be attributed to the *ortho*  $\sigma$  complexes having access to an internal hydrogen bond (in the case of water addition to the *ortho* position of the phenyloxonium ion, geometry optimization leads to a proton transfer from the water to the aryl oxygen apparently without a barrier). The transition states were also computed for return of the *ortho* and *para* Wheland intermediates to the water-bound oxonium ion. Barriers for this back-reaction were found to be reasonably small (11 and 7 kcal/mol, respectively). However, it is also important to consider that a low-barrier tautomerization of the Wheland intermediate to the final aromatic product may effectively render the reaction irreversible. An alternative explanation is that the thermolysis leads to a larger partitioning toward the oxonium ion rather than the radical, leading to more solvent adducts and the differing product ratios. Our preliminary product studies of a protonated hydroxylamine precursor to the biphenyl oxonium ion are suggestive that this latter explanation is more likely to be the correct one.

## CONCLUSIONS

Photolysis of phenylhydroxylamine salt **3** leads to the phenoxy radical as well as a short-lived transient we assign to the phenyloxonium ion. This photoprecursor has a number of advantages, including a simple synthesis and the theoretical possibility to generate other oxonium ions in nonionizing solvents. A derivative of this precursor that cleanly generates oxonium ions in a general way would be a major help in studying the chemistry and properties of these important species.

## MATERIALS AND METHODS

### LFP Experiments. *fs-Transient Absorption (fs-TA) Experiments.*

The fs-TA measurements were performed on the basis of a commercial femtosecond Ti/sapphire regenerative amplifier laser system and Helios Transient Absorption Spectrometer. A flow cell was used in order to prevent the accumulation of photodecomposition products. For the present experiments, the sample solution was excited by a 267 nm pump beam (the third harmonic of 800 nm, the regenerative amplifier fundamental) and probed by a white light continuum produced from a one-dimensional movable  $CaF_2$  plate pumped by the fundamental laser pulses (800 nm). The pump and probe laser beam spot sizes at the sample were about 500 and 200  $\mu m$ , respectively. The detection signals (with and without 267 nm pump) were focused into an optics fiber coupled to a multichannel spectrometer with a CMOS sensor. The time delay between the pump and probe pulse was controlled by an optical delay line, and the instrument response time was  $\sim 200$  fs. The fs-TA experiments were carried out for precursor **3** in neat MeCN and 1/1  $H_2O$ /MeCN with a sample concentration of  $\sim 1 \mu M$ .

*ps-Kerr-Gated-Time-Resolved Resonance Raman (ps-KTR<sup>3</sup>) Experiments.* Briefly, the Ti/sapphire regenerative amplifier laser system was operated in picosecond mode with a 800 nm,  $\sim 1$  ps, and 1 kHz output. Samples were pumped by a 267 nm pulse and probed with a 400 nm pulse. The 267 and 400 nm probe pulses were the third and second harmonics of the regenerative amplifier fundamental, respectively. The pump and probe pulse durations were  $\sim 1.5$  ps; the pulse energies at the sample were 8–10  $\mu J$ . The pump and probe laser beams were lightly focused onto a flowing liquid sample, and the Raman scattering was collected via a backscattering configuration and then focused into the Kerr medium ( $CS_2$  in a 1 mm thickness UV cell) placed at the other focus point of the ellipse. The Kerr medium was placed between a crossed polarizer pair with an extinction coefficient of  $\sim 10^4$ . The gating beam was polarized at  $45^\circ$  and focused to the Kerr medium with an adjusted intensity to create, in effect, a half-waveplate that rotates the polarization of the light from the sample, allowing it to be transmitted through a Glan Taylor polarizer for the duration of the induced anisotropy created by the femtosecond gating pulse. The Raman light that passed through the second polarizer was focused into a monochromator and detected by a liquid  $N_2$  cooled CCD. The wavenumber shifts of the resonance Raman spectra were calibrated using the known MeCN solvent Raman bands, and the spectra presented were obtained from subtraction of an appropriately scaled probe-before-pump spectrum from the corresponding pump–probe spectrum. The ps-KTR<sup>3</sup> measurements were also carried out for BDP in 100% MeCN.

**Product Studies.** Product studies were performed with 5 mg of precursor **3** dissolved in 3 mL of solvent. The sample was degassed before beginning the photolysis, and the sample was irradiated with 254 nm UV light from a mercury vapor lamp for 1 h in a Rayonet photoreactor. The solvent was then removed, and a <sup>1</sup>H NMR spectrum was obtained. Thermolysis studies were performed similarly with 10 mg of precursor **3** and 10 mL of solvent refluxed for 1 h.

**Computational Methods.** For the computational studies, all of the molecular geometries were optimized at the B3LYP/CC-pVTZ level of theory.<sup>52–54</sup> The stationary points were found to have zero imaginary frequencies, and all energies contain a correction for the zero-point energy. Transition states were found to have one imaginary

frequency that connected the starting material and product and included a PCM solvent model for water. The UV spectra were computed using TD-B3LYP/6-311+G(2d,p). The resonance Raman spectra were found using B3LYP/6-31+G(d,p) with a 400 nm incident beam, and all frequencies were scaled by 0.964.<sup>55</sup> All computations were done with Gaussian 09.<sup>56</sup>

## ■ ASSOCIATED CONTENT

### ■ Supporting Information

Text, tables, and figures giving additional LFP experimental data, synthesis details, compound characterization data, NMR product studies, and Cartesian coordinates and absolute energies for computed structures. This material is available free of charge via the Internet at <http://pubs.acs.org>.

## ■ AUTHOR INFORMATION

### Corresponding Author

winter@iastate.edu

### Notes

The authors declare no competing financial interest.

## ■ ACKNOWLEDGMENTS

A.H.W. thanks the Petroleum Research Fund and Cottrell Scholar Award from the Research Corporation for Scientific Advancement for funding. D.L.P. acknowledges funding from the Research Grants Council of Hong Kong (HKU 7048/11P) and the University Grants Committee Special Equipment Grant (SEG-HKU-07). Support from the University Grants Committee Areas of Excellence Scheme (AoE/P-03/08) is also gratefully acknowledged.

## ■ REFERENCES

- (1) Hanway, P. J.; Winter, A. H. *J. Am. Chem. Soc.* **2011**, *133*, 5086.
- (2) Hanway, P. J.; Winter, A. H. *J. Phys. Chem. A* **2012**, *116*, 9398.
- (3) Williams, L. L.; Webster, R. D. *J. Am. Chem. Soc.* **2004**, *126*, 12441.
- (4) Peng, H. M.; Webster, R. D. *J. Org. Chem.* **2008**, *73*, 2169.
- (5) Olah, G. A.; Molnar, A. *Hydrocarbon Chemistry*; Wiley: Hoboken, NJ, 2003.
- (6) Omura, K. *J. Org. Chem.* **1996**, *61*, 7156.
- (7) Omura, K. *J. Org. Chem.* **1996**, *61*, 2006.
- (8) Wenderski, T. A.; Huang, S. L.; Pettus, T. R. R. *J. Org. Chem.* **2009**, *74*, 4104.
- (9) Swenton, J. S.; Carpenter, K.; Chen, Y.; Kerns, M. L.; Morrow, G. W. *J. Org. Chem.* **1993**, *58*, 3308.
- (10) Troisi, F.; Pierro, T.; Gaeta, C.; Neri, P. *Org. Lett.* **2009**, *11*, 697.
- (11) Gamez, P.; Gupta, S.; Reedijk, J. C. R. *Chim.* **2007**, *10*, 295.
- (12) Taylor, W. L.; Battersby, A. R. *Oxidative Coupling of Phenols*; Marcel Dekker: New York, 1967.
- (13) Baesjou, P. J.; Driessen, W. L.; Challa, G.; Reedijk, J. *J. Am. Chem. Soc.* **1997**, *119*, 12590.
- (14) Vigalok, A.; Rytchinski, B.; Gozin, Y.; Koblenz, T. S.; Ben-David, Y.; Rozenberg, H.; Milstein, D. *J. Am. Chem. Soc.* **2003**, *125*, 15692.
- (15) Siuzdak, G.; BelBruno, J. J. *Laser Chem.* **1991**, *11*, 83.
- (16) Reiner, E. J.; Harrison, A. G. *Int. J. Mass Spectrom. Ion Processes* **1984**, *58*, 97.
- (17) Siuzdak, G.; North, S.; BelBruno, J. J. *J. Phys. Chem.* **1991**, *95*, 5186.
- (18) Smith, D. *Chem. Rev.* **1992**, *92*, 1473.
- (19) Leyva, E.; Platz, M. S.; Persy, G.; Wirz, J. *J. Am. Chem. Soc.* **1986**, *108*, 3783.
- (20) Lewis, J.; Prinn, R. *Planets and Their Atmospheres*; Academic Press: New York, 1994.
- (21) Osborne, R. L.; Coggins, M. K.; Raner, G. M.; Walla, M.; Dawson, J. H. *Biochemistry* **2009**, *48*, 4231.
- (22) Zhang, Y.; Kubicki, J.; Wang, J.; Platz, M. S. *J. Phys. Chem. A* **2008**, *112*, 11093.
- (23) Zhang, Y.; Burdzinski, G.; Kubicki, J.; Platz, M. S. *J. Am. Chem. Soc.* **2008**, *130*, 16134.
- (24) Burdzinski, G. T.; Gustafson, T. L.; Hackett, J. C.; Hadad, C. M.; Platz, M. S. *J. Am. Chem. Soc.* **2005**, *127*, 13764.
- (25) Gritsan, N. P.; Tigelaar, D.; Platz, M. S. *J. Phys. Chem. A* **1999**, *103*, 4465.
- (26) Gritsan, N. P.; Gudmundsdottir, A. D. R.; Tigelaar, D.; Zhu, Z.; Karney, W. L.; Hadad, C. M.; Platz, M. S. *J. Am. Chem. Soc.* **2001**, *123*, 1951.
- (27) Wang, J.; Kubicki, J.; Platz, M. S. *Org. Lett.* **2007**, *9*, 3973.
- (28) Xue, J.; Luk, H. L.; Eswaran, S. V.; Hadad, C. M.; Platz, M. S. *J. Phys. Chem. A* **2012**, *116*, 5325.
- (29) Wang, J.; Burdzinski, G.; Zhu, Z.; Platz, M. S.; Carra, C.; Bally, T. J. *J. Am. Chem. Soc.* **2007**, *129*, 8380.
- (30) Hwang, W. G.; Kim, M. S.; Choe, J. C. *J. Phys. Chem.* **1996**, *100*, 9227.
- (31) Kosmidis, C.; Ledingham, K. W. D.; Kilic, H. S.; McCanny, T.; Singhal, R. P.; Langley, A. J.; Shaikh, W. J. *J. Phys. Chem. A* **1997**, *101*, 2264.
- (32) Syage, J. A.; Steadman, J. J. *J. Phys. Chem.* **1992**, *96*, 9606.
- (33) Novak, M.; Glover, S. A. *J. Am. Chem. Soc.* **2004**, *126*, 7748.
- (34) Novak, M.; Brinster, A. M.; Dickhoff, J. N.; Erb, J. M.; Jones, M. P.; Leopold, S. H.; Vollman, A. T.; Wang, Y. T.; Glover, S. A. *J. Org. Chem.* **2007**, *72*, 9954.
- (35) Novak, M.; Glover, S. A. *J. Am. Chem. Soc.* **2005**, *127*, 8090.
- (36) Novak, M.; Poturalski, M. J.; Johnson, W. L.; Jones, M. P.; Wang, Y. T.; Glover, S. A. *J. Org. Chem.* **2006**, *71*, 3778.
- (37) Wang, Y.-T.; Jin, K. J.; Leopold, S. H.; Wang, J.; Peng, H.-L.; Platz, M. S.; Xue, J.; Phillips, D. L.; Glover, S. A.; Novak, M. *J. Am. Chem. Soc.* **2008**, *130*, 16021.
- (38) Wang, Y. T.; Wang, J.; Platz, M. S.; Novak, M. *J. Am. Chem. Soc.* **2007**, *129*, 14566.
- (39) Winter, A. H.; Thomas, S. I.; Kung, A. C.; Falvey, D. E. *Org. Lett.* **2004**, *6*, 4671.
- (40) Baptista, J. L.; Burrows, H. D. *J. Chem. Soc., Faraday Trans. 1* **1974**, *70*, 2066.
- (41) Tripathi, G. N. R.; Schuler, R. H. *J. Chem. Phys.* **1984**, *81*, 113.
- (42) Land, E. J.; Porter, G.; Strachan, E. *Trans. Faraday Soc.* **1961**, *57*, 1885.
- (43) Shindo, H.; Hiraishi, J. *Chem. Phys. Lett.* **1981**, *80*, 238.
- (44) Gritsan, N. P.; Likhovotrik, I.; Zhu, Z.; Platz, M. S. *J. Phys. Chem. A* **2001**, *105*, 3039.
- (45) Delamere, C.; Jakins, C.; Lewars, E. *J. Mol. Struct. (THEOCHEM)* **2002**, *593*, 79.
- (46) Xue, J.; Luk, H. L.; Eswaran, S. V.; Hadad, C. M.; Platz, M. S. *J. Phys. Chem. A* **2012**, *116*, 5325.
- (47) Abramovitch, R. A.; Alvernhe, G.; Bartnik, R.; Dassanayake, N. L.; Inbasekaran, M. N.; Kato, S. *J. Am. Chem. Soc.* **1981**, *103*, 4558.
- (48) Abramovitch, R. A.; Alvernhe, G.; Inbasekaran, M. N. *Tetrahedron Lett.* **1977**, 1113.
- (49) Abramovitch, R. A.; Inbasekaran, M.; Kato, S. *J. Am. Chem. Soc.* **1973**, *95*, 5428.
- (50) Endo, Y.; Shudo, K.; Okamoto, T. *J. Am. Chem. Soc.* **1982**, *104*, 6393.
- (51) Shudo, K.; Orihara, Y.; Ohta, T.; Okamoto, T. *J. Am. Chem. Soc.* **1981**, *103*, 943.
- (52) Lee, C.; Yang, W.; Parr, R. G. *Phys. Rev. B* **1988**, *37*, 785.
- (53) Becke, A. D. *Phys. Rev. A* **1988**, *38*, 3098.
- (54) Becke, A. D. *J. Chem. Phys.* **1993**, *98*, 5648.
- (55) Johnson, R. D., III. NIST Computational Chemistry Comparison and Benchmark Database, NIST Standard Reference Database Number 101, Release 15b, August 2011; <http://cccbdb.nist.gov/>.
- (56) Frisch, M. J., et al. *Gaussian09, version A.02*; Gaussian Inc., Pittsburgh, PA, 2009.